Supplementary Information

Acidity-responsive polyphenol-coordinated nanovaccine for improving tumor immunotherapy via bidirectional reshape of immunosuppressive microenvironment and controllable release of antigen

Huimin Qiu,[#] Shuman Wang,[#] Rimei Huang,[#] Xingyu Liu, Liqun Li, Zheng Liu, Aihui Wang, Shichen Ji, Hong Liang, Bang-Ping Jiang and Xing-Can Shen**

State Key Laboratory for Chemistry and Molecular Engineering of Medicinal Resources, School of Chemistry and Pharmaceutical Sciences, Guangxi Normal University, Guilin, 541004, P. R. China.

#The authors contributed equally to this work.

E-mail: xcshen@mailbox.gxnu.edu.cn;jiangbangping@mailbox.gxnu.edu.cn

Experimental Section

Characterization

The morphology of the samples were characterized by transmission electron microscopy (TEM) (JEM-2100F, JEOL Ltd, Tokyo, Japan). Dynamic light scattering (DLS) measurements were recorded using Malvern Zetasizer Nano ZS-90 (Nano ZS-90, Malvern Instruments, Malvern, UK). Fourier transform infrared (FT-IR) spectra of the samples were characterized using FT-IR spectrometer (Spectrum Two, PerkinElmer, Waltham, MA, USA). Raman spectroscopy was carried out on confocal Raman microscope (in Via Quotation, Renishaw, UK) with 785-nm near-infrared laser excitation. The circular dichroism (CD) spectra using spectropolarimeter system (JASCO, J-810). A confocal laser scanning microscope (CLSM) (Leica TCS SP8 DIVE, Wetzlar, Germany) was used to obtain fluorescence images of the cells. UV-Vis-NIR absorption spectra were recorded with a spectrometer (UV-2600, Shimadzu). Try and Kyn content were acquired on time-of-flight liquid chromatography/mass spectrometry (Q-TOF HPLC-MS, Agilent Technologies, Santa Clara, CA, USA). Binding energy values were collected by X-ray photoelectron spectroscopy using monochromated Al Kα radiation (Nexsa, Thermo Fisher Scientific, Waltham, MA, USA). Temperature and images of the samples were recorded with a MAG 30 Infrared camera (Magnity Electronics, Shanghai, China).

In vivo Immunoassay

For macrophage polarization analysis, the tumors of mice were collected, homogenized in PBS, and filtered to gain singlecell suspension. Then, the cell

suspension of tumors was stained with anti-CD206-FITC, anti-F4/80-APC antibodies for macrophage phenotype analysis by flow cytometry. The content of cytokines (IL-12 and IL-10) in serum was measured using ELISA kits.

To analyze Tregs, the tumors of mice were collected, homogenized in PBS to obtain single-cell suspension, the suspension was stained by anti-CD4-FITC, anti-CD3-APC and anti-FOXP3-PE, analyzed by flow cytometry.

For DCs maturation analysis, the distant tumors of mice were collected, homogenized in PBS, and filtered to gain single-cell suspension. Afterwards, the cell suspension of distant tumors was stained with anti-CD86-PE and anti-CD80-FITC antibodies for DCs maturation analysis by flow cytometry. The content of cytokines (IL-6, IFN-γ and TNF-α) in serum was measured using ELISA kits.

For T cells activation analysis, the distant tumors of mice were collected, homogenized in PBS, and filtered to gain single-cell suspension. Afterwards, the cell suspension of distant tumors was stained with anti-CD8-PE, anti-CD4-FITC and anti-CD3-APC, analyzed by flow cytometry.

To analyze memory T cells, the single cell suspensions harvested from spleen of mice were respectively stained with anti-CD8-PE, anti-CD62-APC and anti-CD44-Brilliant Violet 421 antibodies to differentiate central memory T cells (T_{CM}, $CD8^+CD44^+CD62L^+$) and effector memory T cells (T_{EM}, $CD8^+CD44^+CD62L^-$) by flow cytometry.

In vivo histological examinations and biosafety assessments

For histological analysis, the tumor-bearing mice in different treatment groups were sacrificed at 14 days post-injection, and the vital organs (heart, liver, spleen, lung, and kidney) and tumor tissues were excised, fixed in 4% paraformaldehyde overnight, and embedded in paraffin for H&E staining to observe the histological changes. The tumors were sectioned into slices for terminal deoxynucleotidyl transferase-mediated dUTP-biotin nick end labeling (TUNEL), Ki-67 and H&E staining for histological analysis according to standard protocols.

In vivo immunofluorescence staining

The tumor tissues were also sectioned for CD206, CD4 and CD8 immunofluorescence staining to determine the expression of CD206, CD4 and CD8 in tumor sections.

Anti-metastasis effect of combination therapy

Melanoma C57BL/6 mouse were treated with a unilateral tumor regimen. The tumor on each mouse was removed by surgery at 14 days post treatment. Immunomemory analysis was performed on day 30, and $1´10^6$ B16-OVA cells were administered intravenously via tail vein into each C57BL/6 mouse. After 20 days, the mice were sacrificed, the lungs were extracted and photographed, and the pulmonary metastatic nodules were counted. The lung tissues were also fixed in 4% formaldehyde, embedded in paraffin, sectioned, and stained with hematoxylin-eosin (H&E) for immunohistochemical analysis according to standard protocols.

Supplementary Figures

Fig. S1. The Photos of TA-OVA and Fe^{III}-TA-OVA.

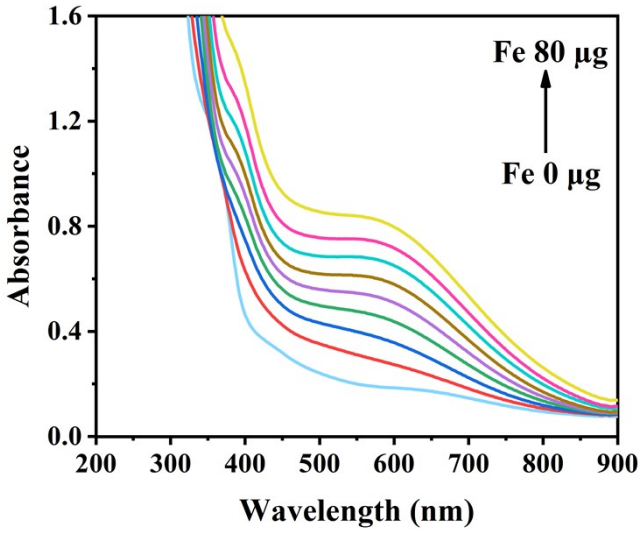

Fig. S2. UV-Vis-NIR absorption spectra of TA-OVA with increasing Fe^{III} content.

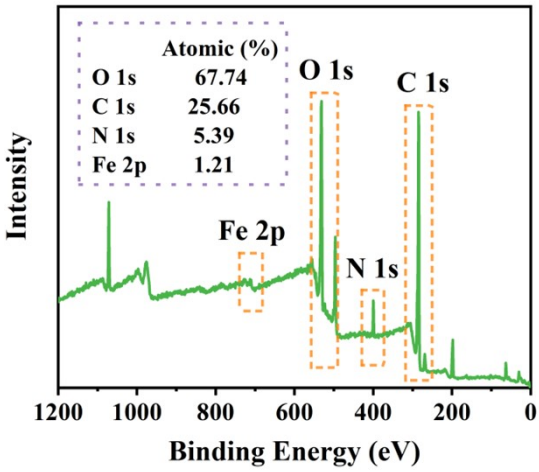

Fig. S3. XPS survey spectrum of Fe^{III}-TA-OVA: survey.

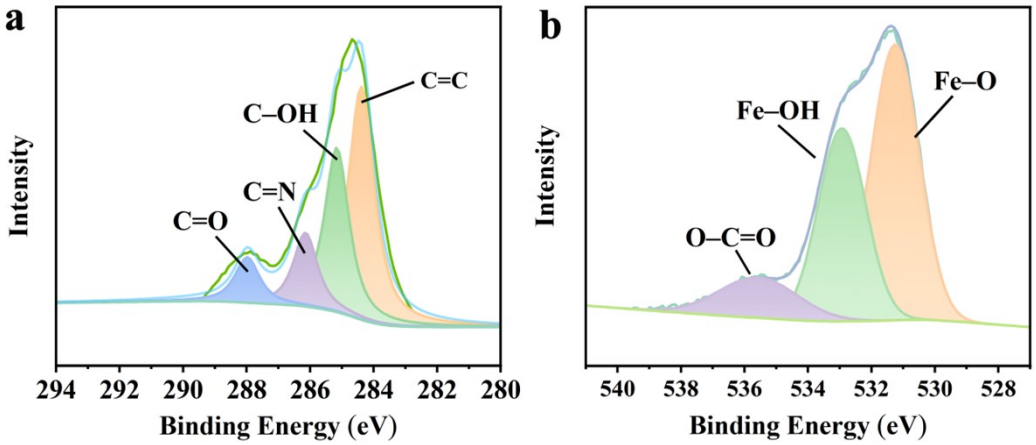

Fig. S4. XPS survey spectrum of Fe^{III}-TA-OVA : (a) C 1s spectra. (b) O 1s spectra.

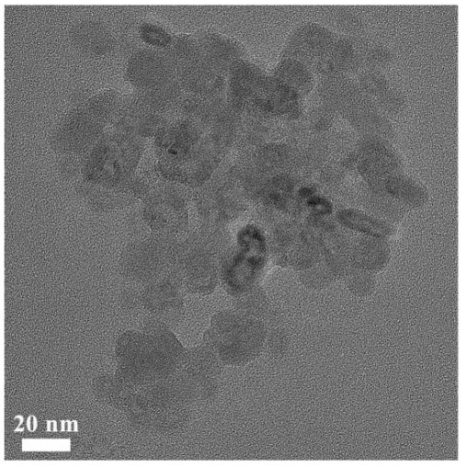

Fig. S5. TEM image of TA-OVA.

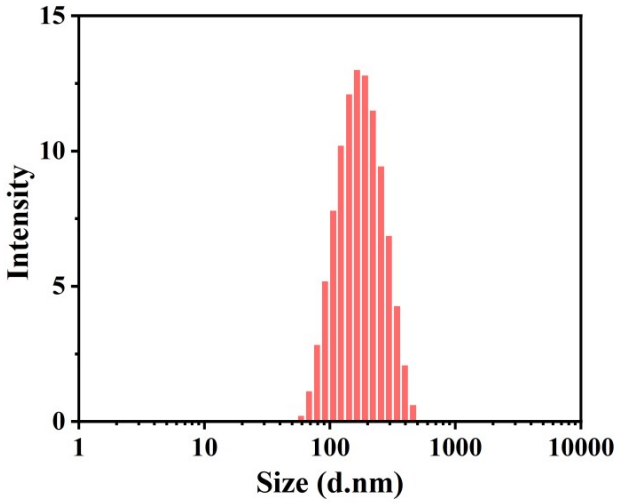

Fig. S6. The hydrodynamic size of Fe^{III}-TA-OVA.

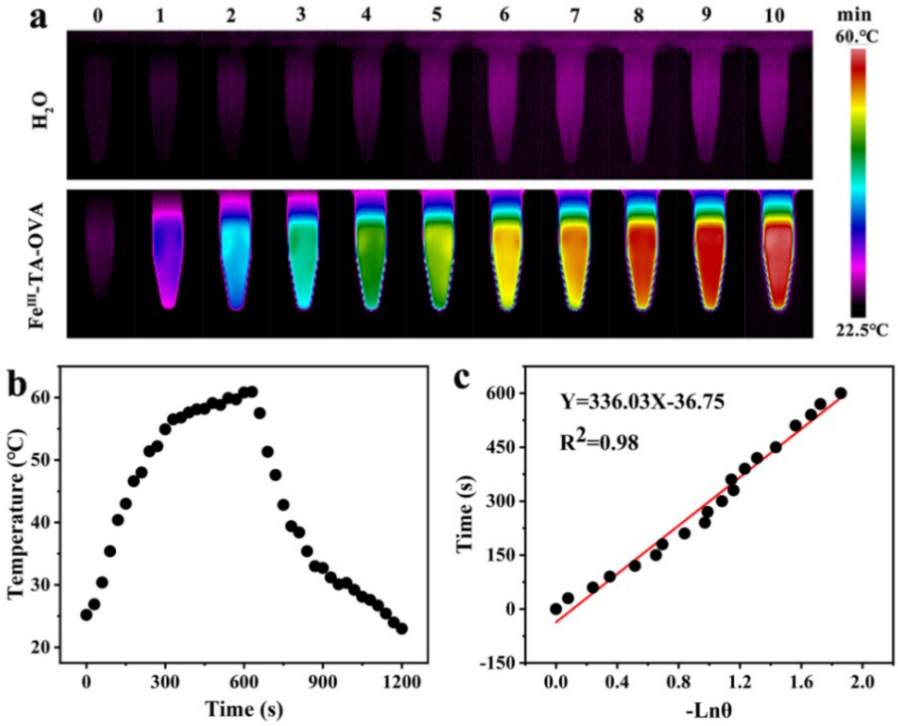

Fig. S7. (a) Photothermal images of Fe^{III}-TA-OVA (500 μg mL^{-1}) and water upon exposure to 808-nm laser (1 W cm^{-2}) for various time periods. (b) The temperature curve of Fe^{III}-TA-OVA (500 μg mL^{-1}) under irradiation (808-nm, 1 W cm^{-2}), and then the laser was removed. (c) Linear time data versus -Lnθ obtained from the cooling period of (b).

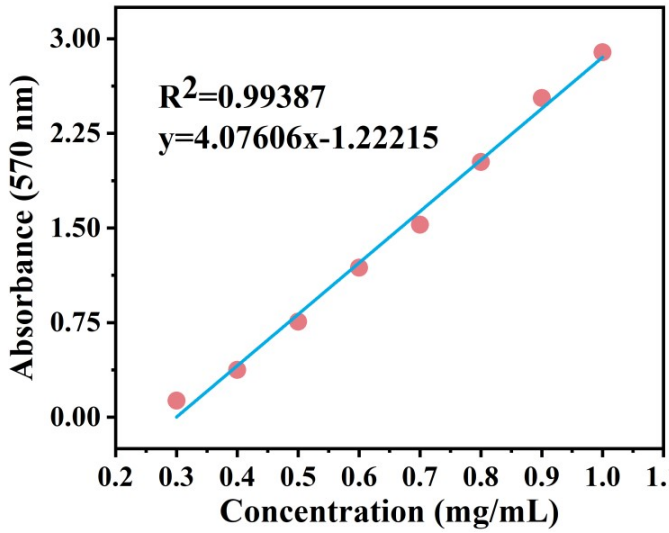

Fig. S8. Standard curve of 1-MT concentration.

Table S1 The content of 1-MT in Fe^{III}-TA-OVA@1-MT, determined using Ninhydrin colorimetry.

NO .	1-MT of Fe^{III}-TA-OVA@1-MT (mg)	Input 1-MT (mg)	Fe^{III}-TA-OVA@1-MT (mg)	Encapsulation Rate (%)	Loading Rate (%)
1	17.7	30	100	59.0	17.7
2	15.5	30	100	51.7	15.5
3	17.0	30	100	56.7	17.0
Average	16.7	30	100	55.8	16.7

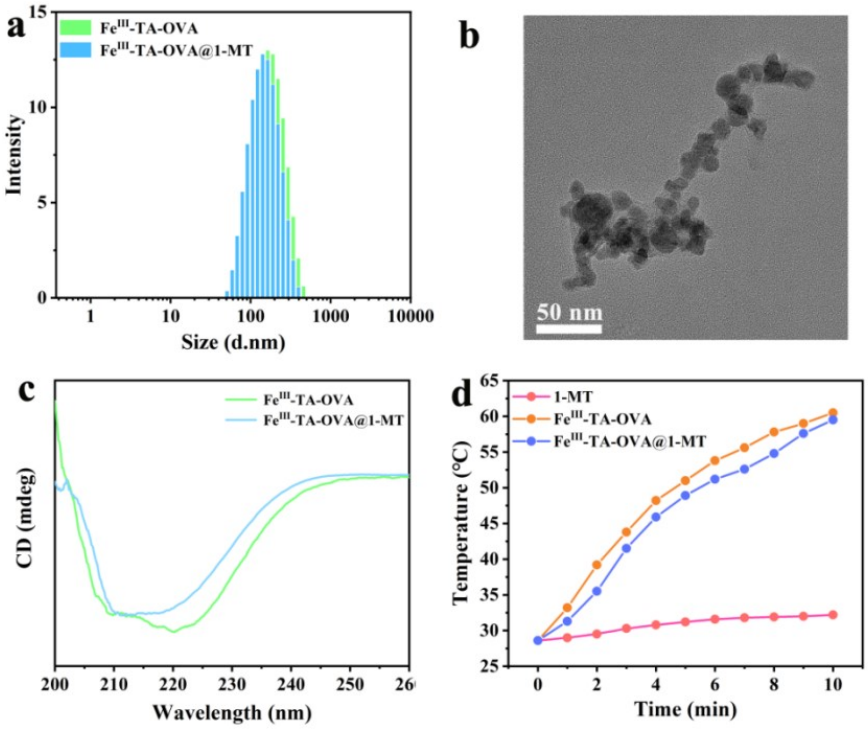

Fig. S9. (a) The hydrodynamic size of Fe^{III}-TA-OVA and Fe^{III}-TA-OVA@1-MT. (b) TEM imaging of Fe^{III}-TA-OVA@1-MT. (c) CD spectrum of Fe^{III}-TA-OVA and Fe^{III}-TA-OVA@1-MT. (d) Photothermal heating curves of different aqueous suspensions of 1-MT, Fe^{III}-TA-OVA and Fe^{III}-TA-OVA@1-MT (500 μg mL^{-1}) under irradiation of 808-nm laser (1 W cm^{-2}).

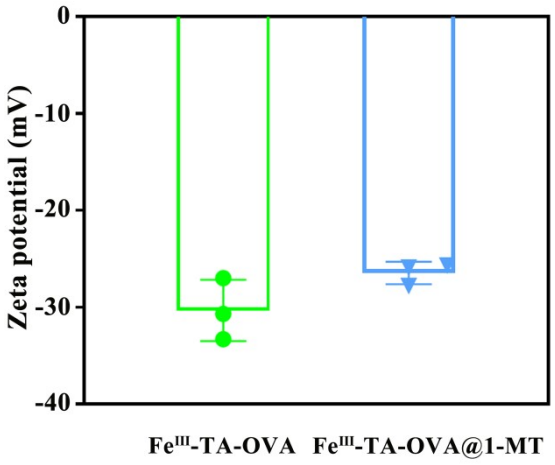

Fig. S10. Zeta potential of Fe^{III}-TA-OVA and Fe^{III}-TA-OVA@1-MT.

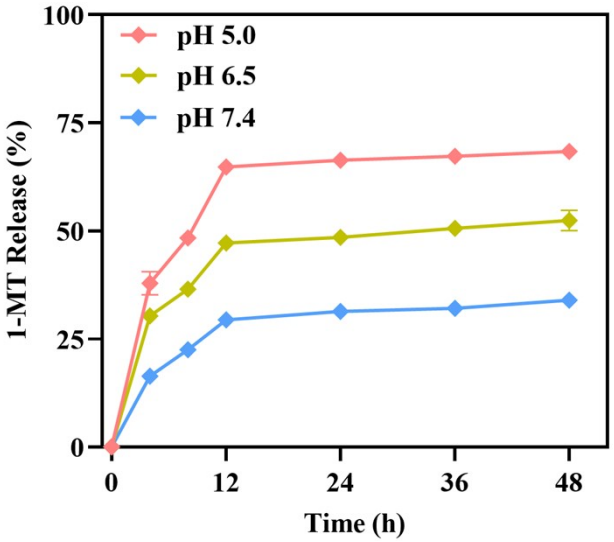

Fig. S11. Release curves of 1-MT from Fe^{III}-TA-OVA@1-MT in PBS with different pH values.

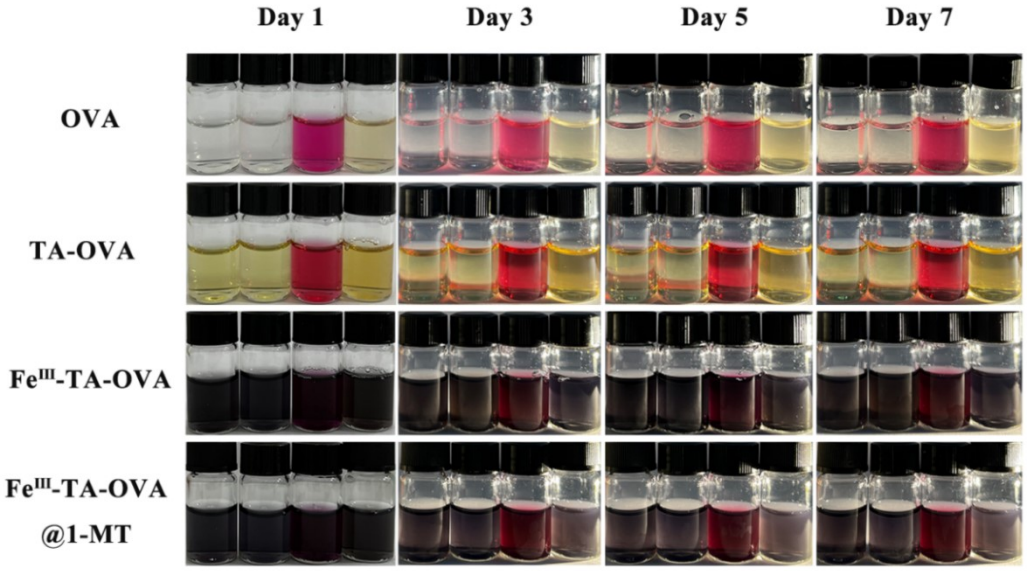

Fig. S12. Pictures of free OVA, TA-OVA, Fe^{III}-TA-OVA and Fe^{III}-TA-OVA@1-MT dispersed in PBS, Saline, DMEM + 10% FBS and FBS solutions for 1, 3, 5 and 7 days.

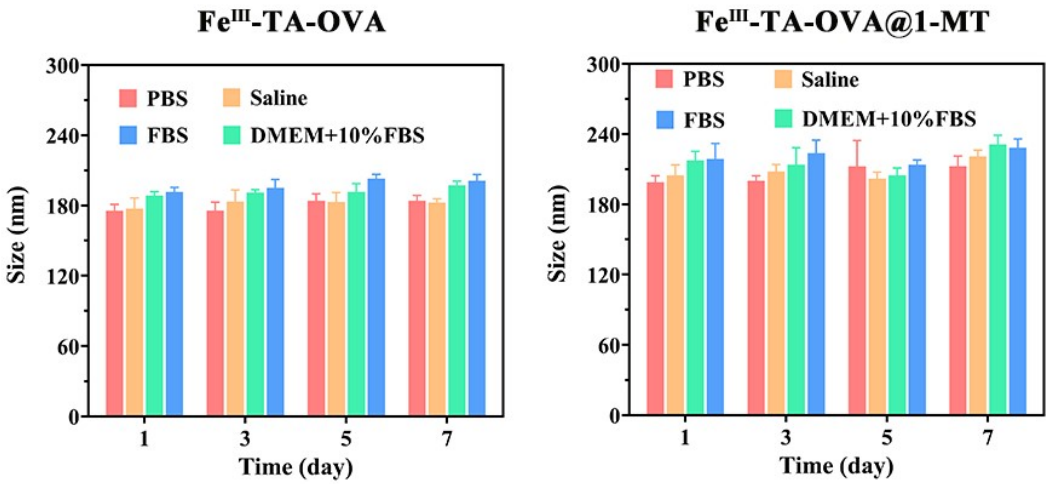

Fig. S13. Time-dependent size of Fe^{III}-TA-OVA and Fe^{III}-TA-OVA@1-MT in PBS, saline, DMEM + 10% FBS and FBS.

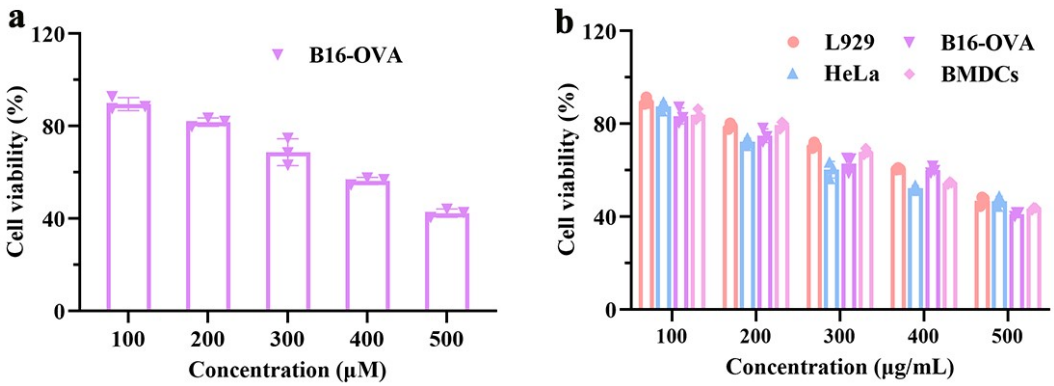

Fig. S14. (a) Relative cell viability of B16-OVA after incubation with Fe^{III}-TA-OVA@1-MT(500 μg mL^{-1}) and pretreatment by different concentrations of H_2O_2. (b) Relative cell viability of L929, HeLa, B16-OVA and BMDCs cells after incubation with different concentrations of Fe^{III}-TA-OVA@1-MT and pretreatment by 500 ⌈M H_2O_2.

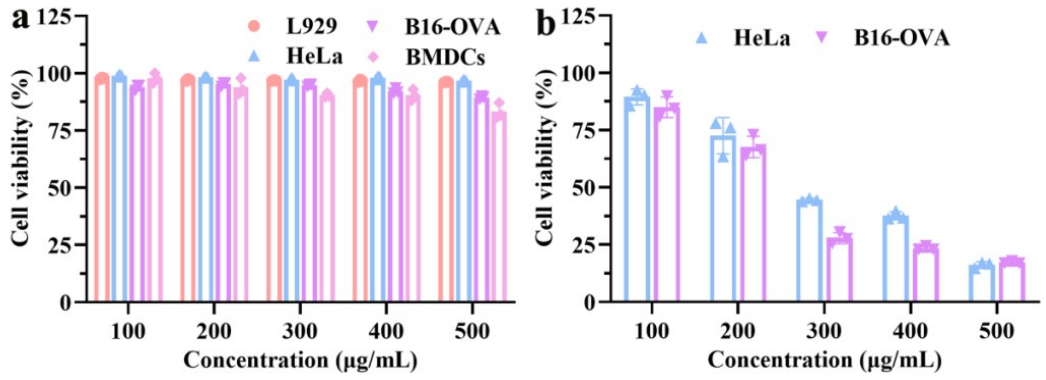

Fig. S15. (a) Relative cell viability of L929, HeLa, B16-OVA and BMDCs cells after incubation with different concentrations of Fe^{III}-TA-OVA. (b) Relative cell viability of HeLa and B16-OVA cells after incubated with different concentrations of Fe^{III}-TA-OVA by laser irradiation. The laser irradiation was performed using 808-nm laser for 5 min (1 W cm^{-2}).

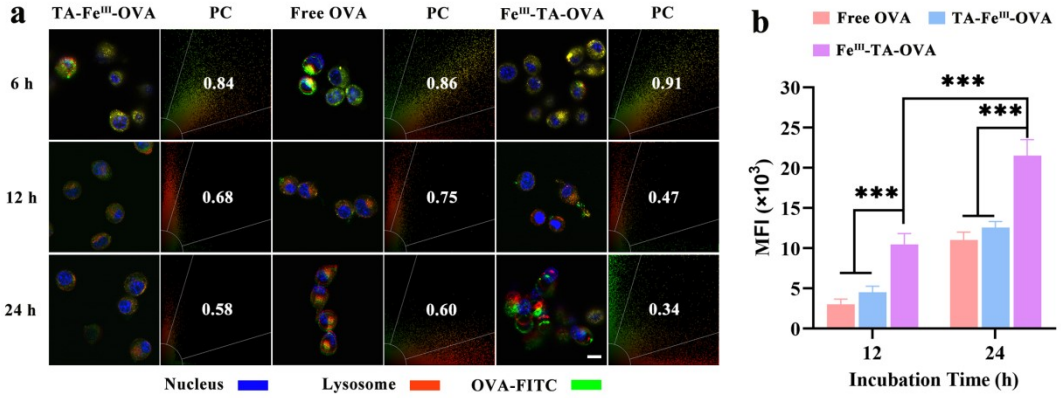

Fig. S16. (a) CLSM images of a LysoTracker colocalization assay performed in B16-OVA cells after incubation for 6, 12 and 24 h with free OVA-FITC, TA-Fe^{III}-OVA-FITC and Fe^{III}-TA-OVA-FITC. Scale bar: 10 μm. (b) Flow cytometry assay results of the intracellular MFI of B16-OVA cells after incubate with free OVA, TA-Fe^{III}-OVA and Fe^{III}-TA-OVA at incubation time (12 and 24 h). All data are presented as mean ± SD (n = 3). ***p < 0.001; **p < 0.01; *p < 0.05.

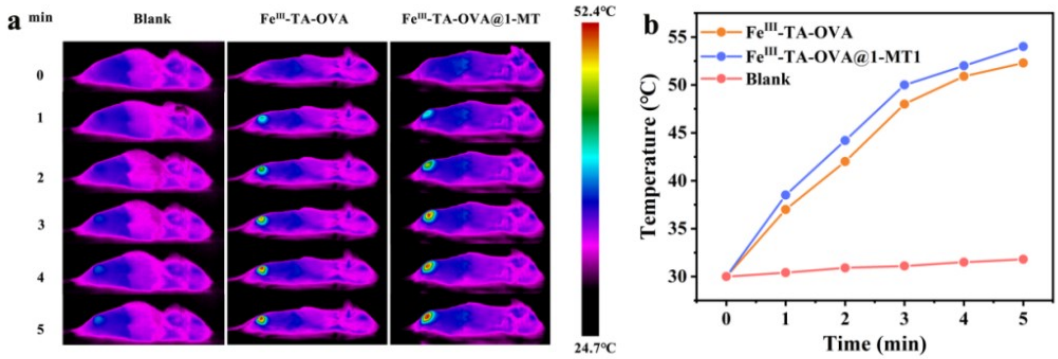

Fig. S17. (a) IR thermal images. (b) Corresponding tumor temperature change curves of B16-OVA tumor mice.

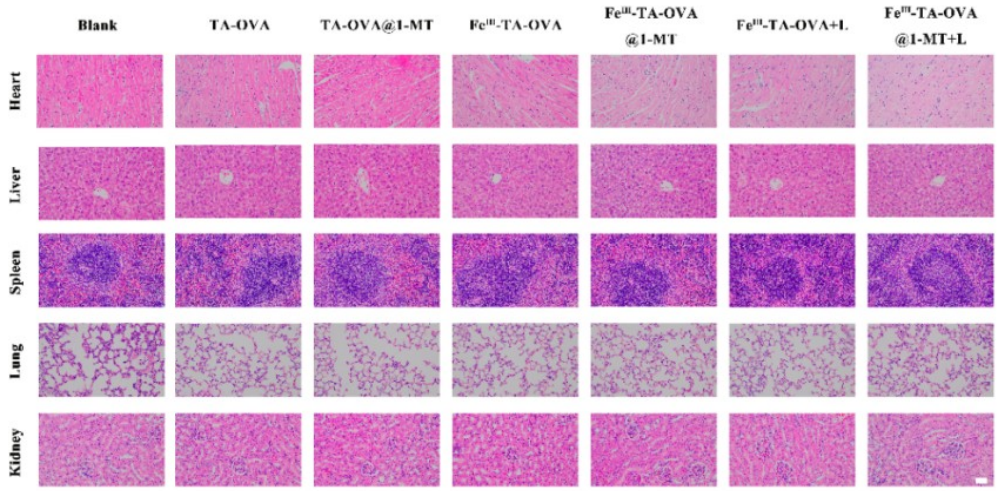

Fig. S18. The main organs of each group were stained by H&E staining. Scale bar: 50 μm.

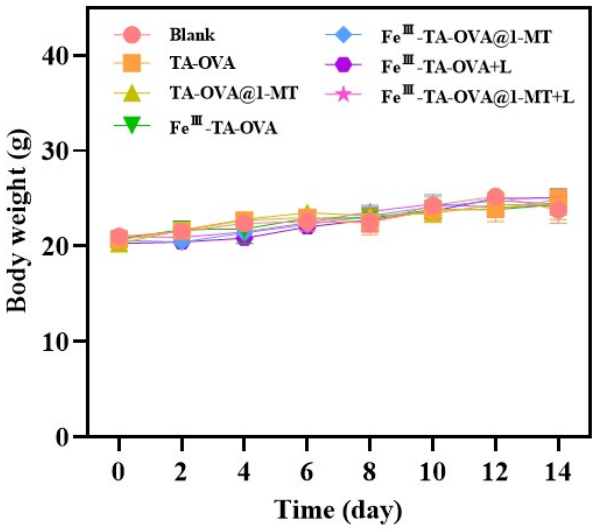

Fig. S19. Body weight curves of the mice during various treatments.

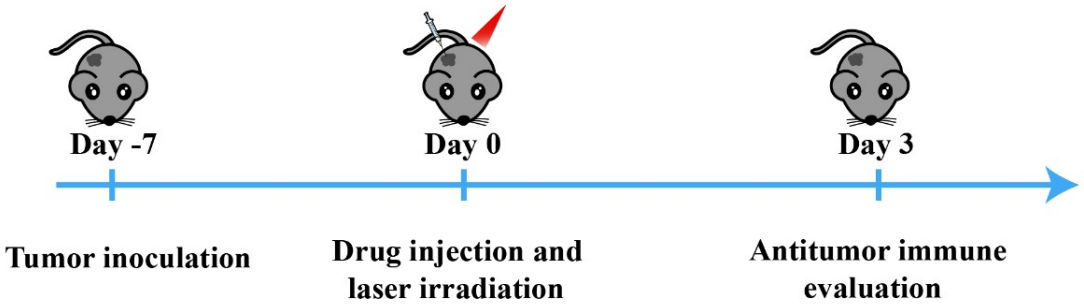

Fig. S20. Schematic illustration of immune effect test *in vitro*.